Movement of the Guide Sequence During RNA Catalysis by a Group I Ribozyme

Jin-Feng Wang, William D. Downs, Thomas R. Cech*

Ribozymes derived from the self-splicing pre–ribosomal RNA of *Tetrahymena* act as sequence-specific endonucleases. The reaction involves binding an RNA or DNA substrate by base pairing to the internal guide sequence (IGS) to form helix P1. Site-specific photo-crosslinking localized the 5′ end of the IGS in helix P1 to the vicinity of conserved bases between helices P4 and P5, supporting a major feature of the Michel-Westhof three-dimensional structure model. The crosslinked ribozyme retained catalytic activity. When not base-paired, the IGS was still specifically crosslinked, but the major site was 37 Å distant from the reactive site in the experimentally supported three-dimensional model. The data indicate that a substantial induced-fit conformational change accompanies P1 formation, and they provide a physical basis for understanding the transport of oligonucleotides to the catalytic core of the ribozyme. The ability of RNA to orchestrate large-scale conformational changes may help explain why the ribosome and the spliceosome are RNA-based machines.

RNA catalysis, originally demonstrated with self-splicing RNAs and ribonuclease P (*1*), now appears to be involved in two key steps of gene expression: messenger RNA (mRNA) splicing and mRNA translation. In mRNA splicing, small nuclear RNAs are involved in recognition of the reaction sites (*2*, *3*) and may participate directly in the chemical steps of the reaction (*2*–*5*). In protein synthesis, the ribosomal RNAs are not simply scaffolds for organization of ribosomal proteins but contribute more directly to the catalysis of translation (*6*, *7*). The substrates for both processes are themselves RNA molecules, and both processes involve multiple conformational changes. RNA may be particularly well suited to catalyze these reactions because it is able to specifically bind substrate RNAs and transfer them substantial distances. While such RNA rearrangements are of fundamental interest, there is very little experimental basis for understanding RNA dynamics. We now present a model system that allows us to monitor an RNA conformational change required for RNA catalysis and to specify in three-dimensional space the structural change that occurs.

The L-21 Sca I ribozyme derived from the self-splicing group I intron of *Tetrahymena thermophila* catalyzes the cleavage of RNA substrates by a transesterification reaction (*8*) (Fig. 1A). Oligonucleotide GGCCCUCUAAAAA, as a substrate, forms a base-paired duplex with the 5′ exon binding site of the ribozyme, GGAGGG, also known as the internal guide sequence (IGS). The 3′ hydroxyl of G (guanosine or one of its 5′-phosphorylated forms) functions as a nucleophile, attacking the phosphate after the sequence CCCUCU. The RNA substrate is cleaved with the concomitant addition of G to the 5′ end of downstream fragment AAAAA. The reaction is analogous to the first step of RNA self-splicing, with the product GGCCCUCU corresponding to the 5′ exon (*9*). Such ribozymes can also specifically cleave single-stranded DNA (*10*, *11*) and an aminoacyl ester attached to the 3′ end of an RNA oligonucleotide (*12*).

The three-dimensional structural model of the *Tetrahymena* ribozyme developed by Michel and Westhof (*13*) provides the necessary structural framework for our studies of RNA dynamics. The overall architecture of the RNA proposed in their model has withstood the test of independent physical and genetic experiments with only a limited amount of adjustment required (*14*–*16*). Our data (shown below) provide a key tertiary structural constraint for this ribozyme, which again supports the Michel-Westhof model. Although the model concerns only one conformational state of the ribozyme, there is good evidence that its overall three-dimensional structure is largely the same with and without the RNA substrate or 5′ exon analogue bound to the IGS (*17*–*19*). Thus, when we use site-specific photo-crosslinking to monitor the location of the IGS in different stages of the catalytic cycle, we can use the three-dimensional model to assign physical distances to the changes we observe.

Site-specific photo-crosslinking. An azidophenacyl group was tethered to the 5′ phosphate of G22 at the 5′ end of the IGS (Fig. 1B) (*20*). The location of G22 is of special interest because it is a phylogenetically invariant nucleotide that is juxtaposed to the uridine at position minus one (U-1) immediately preceding the cleavage site (Fig. 1A). When irradiated in the ultraviolet, the azido moiety is converted to a highly reactive nitrene that either forms a crosslink to a nucleotide in its vicinity or is quickly quenched by solvent (*21*–*23*).

Irradiation of 5′-azido L-21 Sca I RNA in the presence of a saturating concentration of 5′ exon analogue, which forms base pairs with the IGS, gave predominantly a single crosslinked species (1) (Fig. 2A, lanes 3 and 6). A second minor photoproduct, denoted by an asterisk in Fig. 2A, did not depend on the azidophenacyl moiety; this intramolecular crosslink was studied previously (*18*).

Control experiments verified that

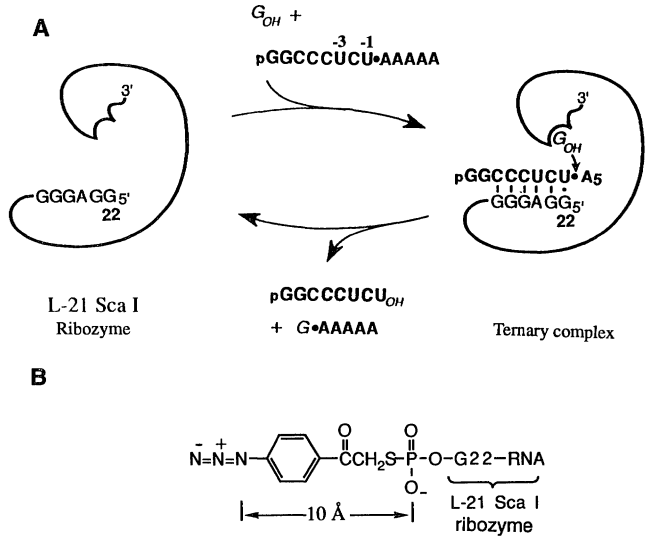

Fig. 1. (**A**) Endonuclease reaction catalyzed by the ribozyme. The RNA substrate (GGCCCUCUAAAAA) forms base pairs with the 5′ exon-binding site (GGAGGG), which is the IGS of the ribozyme. After ribozyme-catalyzed cleavage by guanosine (italic G), the same base pairs persist before oligonucleotide GGCCCUCU (5′ exon analogue) dissociates from the IGS. (**B**) The azidophenacyl group coupled to the 5′ end of the ribozyme through a thiophosphate.

The authors are at the Howard Hughes Medical Institute, Department of Chemistry and Biochemistry, and Department of Molecular, Cellular and Developmental Biology, University of Colorado, Boulder, CO 80309.

*To whom correspondence should be addressed.

crosslinked product **1** resulted from an intramolecular crosslink involving the azido group at the 5′ end of G22. This crosslinked product was not observed after irradiation of unmodified L-21 Sca I RNA (Fig. 2A, lane 9), an indication that the azido group at G22 participated in the crosslinking reaction. Furthermore, the yield of the crosslinked product did not change significantly over a large variation in the concentration of 5′-azido L-21 Sca I RNA (~2 nM to 10 μM), showing that the crosslinking was first order in RNA and therefore suggesting an intramolecular reaction. This was confirmed by the absence of this crosslink product when ^{32}P-labeled underivatized L-21 Sca I RNA was irradiated in the presence of unlabeled 5′-azido L-21 Sca I RNA (Fig. 2A, lane 10). Therefore, an intramolecular crosslink occurs between the nitrene derived from the azido group at G22 and another nucleotide that is in proximity in the folded structure. Because the crosslink involves the 5′ end of the ribozyme, the crosslinked RNA should have a lariat structure (a circle with a tail), which explains its retarded migration in a denaturing gel (*24*).

In the absence of the 5′ exon analogue, irradiation of 5′-azido L-21 Sca I RNA gave two predominant crosslinked products (**2a** and **2b**) (Fig. 2A, lane 4). Neither of these bands comigrated with that produced in the presence of the 5′ exon analogue; they represent crosslinks between the derivatized G22 and two different sites in the ribozyme (see below). In a titration experiment with increasing oligonucleotide concentration, the yields of crosslinks **2a** and **2b** decreased as the yield of crosslink **1** increased (Fig. 2B). The crosslink products formed either in the presence or in the absence of 5′ exon analogue were observed whether or not guanosine was present (Fig. 2A, lane 7) (*19*). Thus, it is the formation of the P1 helix that determines the location of the IGS relative to other parts of the ribozyme.

In the absence of Mg^{2+}, neither crosslink **2a** nor **2b** was formed; instead a new crosslink (**3**) was produced (Fig. 2A, lane 5). Crosslink **3** was also formed with similar efficiency in the presence of the 5′ exon analogue (3 μM) at Mg^{2+} concentrations ≤0.75 mM (*19*). The dependence of crosslinks **1**, **2a**, and **2b** on Mg^{2+} is expected if they reflect tertiary structures of the ribozyme relevant to catalysis because proper folding and catalytic activity of the ribozyme require Mg^{2+} (*15, 18, 25*).

Which of the crosslinks reflects a catalytically active structure? This question was directly assessed by measuring the endonuclease activity of the purified crosslinked RNAs (Table 1). The introduction of the azidophenacyl group at G22 did not affect the cleavage activity of the ribozyme. Furthermore, the value of $(k_{cat}/K_m)^S$ for crosslinked form **1** was only two times lower than that of the uncrosslinked ribozyme (*26, 27*). In contrast, the RNA with crosslinks **2b** and **3** had only 2 and 10 percent the activity of the uncrosslinked ribozyme, respectively. These values are similar to or less than the amount of the uncrosslinked RNA contaminating these preparations (Table 1). This uncrosslinked RNA was probably produced by reversal of the crosslink, as evidenced by its normal mobility on a denaturing gel and, in the case of the uncrosslinked ribozyme derived from the **2a** species, by the same endonuclease activity as the uncrosslinked L-21 Sca ribozyme (*19*). Thus, while we cannot exclude the possibility that the **2b** and **3** species have a small amount of residual catalytic activity, the data do not provide any evidence for such activity. Because the **2a** crosslink was so readily reversed, we hesitate to derive any conclusion about the activity of that crosslinked form.

Using primer extension by reverse transcriptase (*28*), we identified the nucleotides to which the nitrene group at G22 was crosslinked. The major crosslink sites were **1** (A114, A115); **2a** (A87, A88, A89); **2b** (C298, A299, U300, A301); and **3** (U101, C102, A103) (Fig. 3). The retardation of these crosslinked RNAs on a denaturing gel

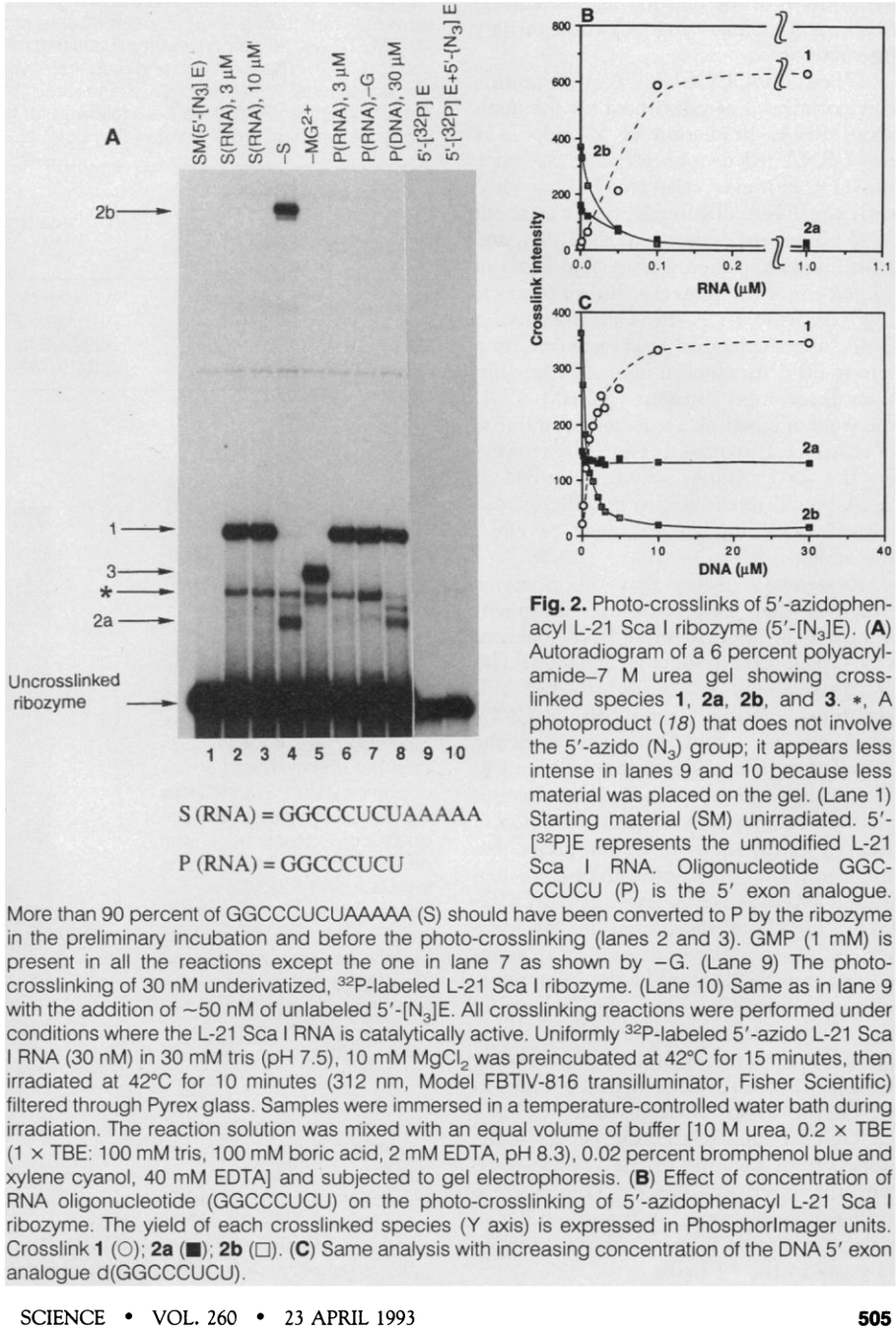

Fig. 2. Photo-crosslinks of 5′-azidophenacyl L-21 Sca I ribozyme (5′-[N_3]E). (**A**) Autoradiogram of a 6 percent polyacrylamide–7 M urea gel showing crosslinked species **1**, **2a**, **2b**, and **3**. *, A photoproduct (*18*) that does not involve the 5′-azido (N_3) group; it appears less intense in lanes 9 and 10 because less material was placed on the gel. (Lane 1) Starting material (SM) unirradiated. 5′-[^{32}P]E represents the unmodified L-21 Sca I RNA. Oligonucleotide GGCCCUCU (P) is the 5′ exon analogue. More than 90 percent of GGCCCUCUAAAAA (S) should have been converted to P by the ribozyme in the preliminary incubation and before the photo-crosslinking (lanes 2 and 3). GMP (1 mM) is present in all the reactions except the one in lane 7 as shown by –G. (Lane 9) The photo-crosslinking of 30 nM underivatized, ^{32}P-labeled L-21 Sca I ribozyme. (Lane 10) Same as in lane 9 with the addition of ~50 nM of unlabeled 5′-[N_3]E. All crosslinking reactions were performed under conditions where the L-21 Sca I RNA is catalytically active. Uniformly ^{32}P-labeled 5′-azido L-21 Sca I RNA (30 nM) in 30 mM tris (pH 7.5), 10 mM $MgCl_2$ was preincubated at 42°C for 15 minutes, then irradiated at 42°C for 10 minutes (312 nm, Model FBTIV-816 transilluminator, Fisher Scientific) filtered through Pyrex glass. Samples were immersed in a temperature-controlled water bath during irradiation. The reaction solution was mixed with an equal volume of buffer [10 M urea, 0.2 × TBE (1 × TBE: 100 mM tris, 100 mM boric acid, 2 mM EDTA, pH 8.3), 0.02 percent bromphenol blue and xylene cyanol, 40 mM EDTA] and subjected to gel electrophoresis. (**B**) Effect of concentration of RNA oligonucleotide (GGCCCUCU) on the photo-crosslinking of 5′-azidophenacyl L-21 Sca I ribozyme. The yield of each crosslinked species (Y axis) is expressed in PhosphorImager units. Crosslink **1** (○); **2a** (■); **2b** (□). (**C**) Same analysis with increasing concentration of the DNA 5′ exon analogue d(GGCCCUCU).

correlated with the expected sizes of the loops created by crosslinks between the derivatized G22 and these identified nucleotides. This provides additional evidence that the stop points for reverse transcription represent the crosslinks, as opposed to the stop point reflecting some other lesion in the RNA and the crosslink residing elsewhere.

Crosslinking the DNA-ribozyme complex. Equilibrium binding of a DNA 5′ exon analogue d(GGCCCUCU) is about 10^4 times weaker at 42°C than the binding of the corresponding RNA oligonucleotide, mainly because of the absence of tertiary interactions with positions −2 and −3 that occur with RNA (*11, 16, 29*). Site-specific crosslinking provides a means of analyzing the position of the IGS in oligonucleotide-ribozyme complexes that lack these tertiary interactions.

When d(GGCCCUCU) at saturating concentration was substituted for the analogous RNA, irradiation of 5′-azido L-21 Sca I RNA led to a crosslink at the same site (**1**). However, the crosslinking yield with the DNA oligonucleotide was about 50 to 60 percent of that with the RNA, and crosslink **2a** appeared with a yield of about 25 percent of the total crosslinked products (Fig. 2A, lane 8). As the concentration of DNA oligonucleotide was increased from zero to 30 μM, which is above the equilibrium dissociation constant (~2 μM) (*30*), the yield of crosslink **2b** decreased and that of crosslink **1** increased (Fig. 2C). However, the **2a** crosslink, which decreased as RNA bound to the IGS (Fig. 2B), instead remained essentially unchanged as DNA was added.

It seemed possible that the ribozyme structure that gave crosslink **2a** might somehow be able to bind RNA but not DNA. The occurrence of an intermolecular crosslink provided a means to test this possibility. With bound d(GGCCCUCUA$_n$, n = 1, 3, and 5), the nitrene at the 5′ end of the IGS underwent crosslinking to the downstream adenosines of the oligonucleotide, as long as the adenosines were not cleaved by the ribozyme during preincubation and the photo-crosslinking. When d(GGCCCUCUAAAAA) or d(GGCCCUCUA) was substituted for d(GGCCCUCU), the minor crosslink (**2a**) disappeared and was replaced by the intermolecular crosslink (*19*). Thus, the **2a** form of the ribozyme is indeed able to bind DNA, providing evidence against the model being tested. Instead, the data support a model in which the minor crosslink with d(GGCCCUCU) bound to the IGS occurs at the same site as **2a**, one of the two observed with the unbound IGS (*28*). Thus, there is evidence for one position that the IGS can occupy either as a single strand or when engaged in the P1 helix.

Guide sequence location in the ribozyme. Our observation of an efficient crosslink between the nitrene group tethered to the 5′ end of the IGS and the A114-A115 site leads to the conclusion that these positions are in proximity in the folded three-dimensional structure of the ribozyme in its reactive form, that is, with the exon analogue bound. This crosslinked RNA (**1**) retains catalytic activity, demonstrating that this location of the IGS is compatible with catalytic function.

Table 1. Summary of crosslinks and relative endonuclease activity of the crosslinked ribozymes. The concentration of Mg^{2+} is either 10 mM (+) or zero (−). The oligo (5′ exon analogue RNA) concentration is 3 μM (+) or zero (−). Crosslink yield (X-L yield), determined by direct scanning of radioactivity in dried gels with a PhosphorImager (Molecular Dynamics), varied less than 10 percent from one experiment to another. Both crosslinking and activity measurements were at 42°C. $(k_{cat}/K_m)^S_{rel}$ is defined as $(k_{cat}/K_m)^S_{X\text{-}L}/(k_{cat}/K_m)^S_{un\text{-}X\text{-}L}$, the ratio of the $(k_{cat}/K_m)^S$ measured with the crosslinked species to the value with the uncrosslinked 5′-azidophenacyl L-21 Sca I ribozyme; $(k_{cat}/K_m)^S_{un\text{-}X\text{-}L}$ was 3.2×10^7 M^{-1} min^{-1}. All values of $(k_{cat}/K_m)^S$ were measured under single-turnover conditions (*27*), with an excess of ribozyme (10 nM) and trace amount of oligoribonucleotide substrate (~1 nM). Reactions were initiated by addition of the 5′-[^{32}P] end-labeled substrate (GGCCCUCUAAAAA) after a 15-minute preliminary incubation of L-21 Sca I RNA with 10 mM $MgCl_2$, 30 mM tris (pH 7.5), and 0.6 mM guanosine or GMP at 42°C. Typically eight portions of 1 μl were removed from a 20-μl reaction mixture at specified times and quenched with four volumes of 40 mM EDTA in 90 percent formamide with 0.01 percent bromphenol blue and xylene cyanol, 1 mM tris (pH 7.5). The product and substrate were separated by electrophoresis on 20 percent polyacrylamide–7 M urea gels, and their ratio at each time point was quantitated with a PhosphorImager. Reactions were followed for five half-lives, within which the disappearance of the substrate was first order, with an end point of ~5 percent corresponding to unreactive substrate.

X-L	Conditions		Locations	X-L yield (%)	Activity	
	Mg^{2+}	Oligo			$(k_{cat}/K_m)^S_{rel}$	Reversed (%)
1	+	+	A114/A115	34	0.47	9
2a	+	−	A87/A88/A89	12	0.80	57
2b	+	−	A299/U300/A301	23	0.02	7
3	−	±	C102/A103/A104	38	0.09	8

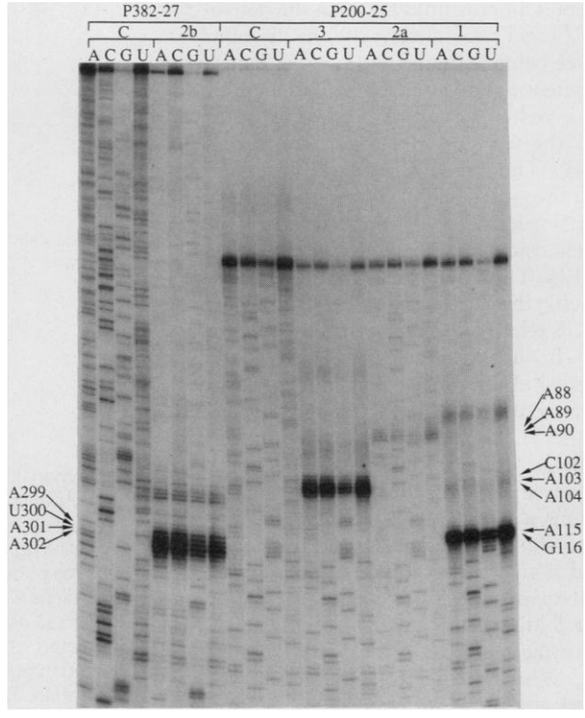

Fig. 3. Primer extension analysis of the nucleotides crosslinked to the nitrene at the 5′ end of L-21 Sca I RNA. P382-27 and P200-25 denote 27-nucleotide and 25-nucleotide primers used in those sequencing lanes and complementary to nucleotides 383 to 409 and 201 to 225 of L-21 Sca I RNA, respectively. (Lanes C) Dideoxynucleotide-terminated sequencing reactions with irradiated but uncrosslinked 5′-azidophenacyl L-21 Sca I RNA as the template; (lanes **2b**) sequencing reactions with crosslinked **2b** RNA as the template and P382-27 as the primer; (lanes **3**, **2a**, and **1**) sequencing reactions with crosslinked species **3**, **2a**, and **1**, respectively, as templates and P200-25 as the primer. The arrows indicate the nucleotide positions at which reverse transcriptase procession is halted by crosslinks. The crosslink positions are assigned as shifted one nucleotide to the 5′ end of these stop sites. Gel-purified ribozyme (0.2 to 0.5 pmol) was hybridized with 1 pmol 5′ end-labeled primer. Primers were extended with AMV reverse transcriptase for 1 hour at 50°C in the presence of all four dNTP's (deoxynucleoside triphosphates, 400 μM each) and a single ddNTP (dideoxynucleoside triphosphate, 80 μM). The products were resolved by electrophoresis on an 8 percent polyacrylamide–7 M urea gel; an autoradiogram of one such gel is shown.

Because G22 is not forced to be in proximity to the A114-A115 site by the RNA secondary structure (Fig. 4A), the proximity of these sites in the folded molecule provides a key structural constraint for the tertiary architecture of this catalytic group I intron. In agreement with our observation, the model proposed by Michel and Westhof (*13*) for the 3D structure of group I introns shows A114 and A115 as the closest nucleotides to G22 (6.7 Å, N1 of A114 or A115 to 5′P of G22). Michel and Westhof modeled the second step of self-splicing, where the cleaved 5′ exon is bound to the IGS; therefore their model is compared to the crosslink observed with the 5′ exon analogue bound.

A114 and A115 are among the most phylogenetically conserved nucleotides of group I introns (99 and 63 percent, respectively, of 87 group I introns analyzed in (*13*), and therefore it seems likely that they have conserved roles in the structure and function of these catalytic RNAs. Although the observation of a crosslink indicates proximity and not necessarily direct tertiary contact between G22 and A114 or A115, some tertiary interaction may exist between them (*13*). Consistent with such a role, mutation or deletion of A114 inhibits the G addition reaction of the ribozyme (*16*, *31*); in contrast, mutations in A114 do not have much effect on 3′ splice site hydrolysis, a reaction that does not appear to involve the IGS (*32*). Nucleotide A207, located across the P4-P5 loop from A114-A115, was previously shown to be in proximity to the 5′ end of the bound guanosine nucleophile (*15*). We therefore propose that the P4-P5 loop is a structural host for the cleavage reaction, helping to position the guanosine nucleophile bound in P7 relative to the reaction site across from G22.

Conformational change on binding oligonucleotide. The 5′ end of the IGS crosslinks to different sites depending on the presence or absence of the 5′ exon analogue, an indication that a conformational change accompanies the binding of this oligonucleotide. The free IGS is at positions where G22 is close to the A88 or the U300 site. After the oligonucleotide binds to the IGS to form the P1 duplex, G22 is positioned close to A114 and A115. In the Michel-Westhof model, U300 is 36.7 Å from A114 (Fig. 4B). Thus, even though each position has a maximum uncertainty of ±10 Å because of the length of the azidophenacyl crosslinking agent (Fig. 1B), the conformational change must be a large-distance movement of P1, not just a local adjustment. Furthermore, because the main architecture of the ribozyme appears to be independent of whether P1 is formed or not (*17*–*19*), it is likely that the conformational change is limited to the movement of the IGS. The A88 site in P2.1 was not modeled by Michel and Westhof, but may lie close to the A114 site (Fig. 4B).

There is evidence that the transport of the unbound oligonucleotide in solution to the catalytic core of the ribozyme involves at least two separate steps (*33*, *34*). First, the oligonucleotide binds to the IGS by base pairing to form an "open complex." Interactions between the newly formed duplex (P1) and other portions of the ribozyme then result in a "closed complex," with P1 positioned at the proper site for nucleophilic attack by guanosine bound at the G site. This docking of P1 into the catalytic core can be considered to be an induced-fit conformational change (*33*), as has been characterized for protein enzymes (*35*). The change in crosslinking that we observe upon addition of RNA oligonucleotide reflects the movement of the free IGS (states **2a** and **2b**) to the closed complex (state **1**). We would not expect there to be a significant population of the intermediate open complex, because the equilibrium so much favors the final closed complex (*33*, *34*, *36*). With bound DNA, however, we observe about 25 percent of the crosslink

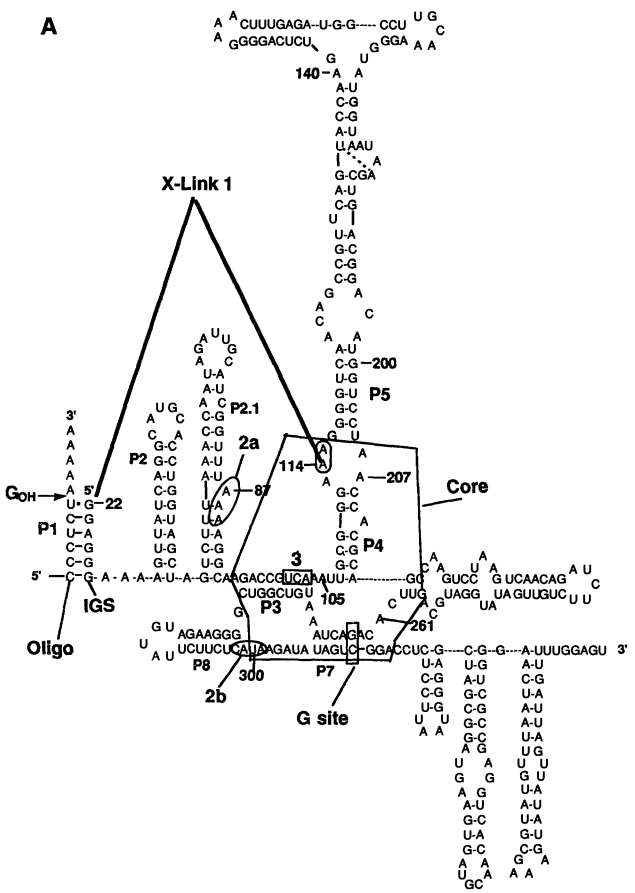

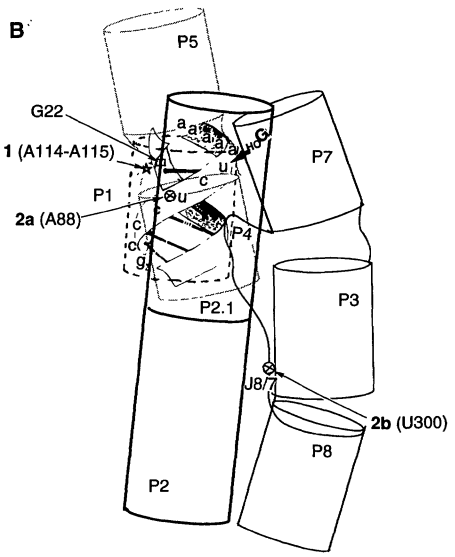

Fig. 4. Sites of crosslinking by the nitrene group tethered to the 5′ end of the L-21 Sca I ribozyme. (**A**) Sites superimposed on the secondary structure diagram of the RNA (*13*). **1**, positions of crosslinks observed in the presence of 5′ exon analogue. **2a** and **2b**, positions of crosslinks in the absence of the 5′ exon analogue. **3**, crosslinks produced in the absence of Mg^{2+}. (**B**) Schematic representation of the extended three-dimensional model of the core of the *Tetrahymena* intron (*13*) with P2.1 included (*18*). P1 is represented by the dash-lined cylinder residing in a cleft surrounded by P2.1, J8/7, P7, P4, and the P4-P5 loop. P2.1 lies on top of P1 as represented by the thick lines, and P4, the P4-P5 loop, and P5 are behind P1 as represented by the light lines. In the absence of the 5′ exon analogue, the 5′ end of the ribozyme crosslinks mainly to the U300 site (~67 percent; 33 percent to A88 site). The shortest distance between the A114 and U300 base moieties is 36.7 Å. The A88 site in P2.1 appears to lie close to the A114 site.

still occurring between the 5′ end of the IGS and the A88 site (A87, A88, A89) even at saturating DNA concentration. With bound DNA, the equilibrium lies more in the direction of the open complex (37); the crosslink at the A88 site may represent this open complex. This would mean that the P1 duplex is not disordered in the open complex, but rather it is specifically positioned relative to the ribozyme core. According to this model, the successive movement of the IGS required for ribozyme activity would be from states **2a** and **2b** (free IGS) → state **2a** (P1 formed, open complex) → state **1** (closed complex). In addition to supporting the two-step binding model, our study gives it a physical reality by identifying the locations of the IGS during the binding process.

In conclusion, the IGS is positioned at specific sites during the ribozyme reaction. The transport of the unbound oligonucleotide from solution to the catalytic core is accompanied by a large-distance reorganization of the IGS relative to the catalytic core. RNA being particularly well suited to large conformational changes with low activation energy has been proposed previously (38). Large-scale RNA conformational changes are thought to be involved in mRNA splicing, which involves the assembly and disassembly of small nuclear ribonucleoproteins (snRNPs) with each other and with the pre-mRNA (39). Protein synthesis requires movement of mRNA, tRNA, and rRNA relative to each other (6). Both of these cellular processes occur in ribonucleoprotein complexes, the protein components of which certainly participate in facilitating conformational changes (2). Nevertheless, the RNAs by themselves may be able to undergo many of the requisite conformational changes, as evidenced by our results presented here concerning RNA catalysis in the absence of protein. This may in part explain why the spliceosome and the ribosome remain RNA machines.

REFERENCES AND NOTES

1. K. Kruger *et al.*, *Cell* **31**, 147 (1982); C. Guerrier-Takada *et al.*, *ibid.* **35**, 849 (1983); A. J. Zaug and T. R. Cech, *Science* **231**, 470 (1986).
2. C. Guthrie, *Science* **253**, 157 (1991).
3. J. A. Steitz, *ibid.* **257**, 888 (1992).
4. T. R. Cech, *Cell* **44**, 207 (1986).
5. P. Fabrizio and J. Abelson, *Science* **250**, 404 (1990); H. D. Madhani and C. Guthrie, *Cell* **71**, 803 (1992); D. S. McPheeters and J. Abelson, *ibid.* **71**, 819 (1992).
6. H. F. Noller, *Annu. Rev. Biochem.* **60**, 191 (1991).
7. H. F. Noller, V. Hoffarth, L. Zimniak, *Science* **256**, 1416 (1992).
8. A. J. Zaug, M. D. Been, T. R. Cech, *Nature* **324**, 429 (1986); A. J. Zaug, C. A. Grosshans, T. R. Cech, *Biochemistry* **27**, 8924 (1988).
9. T. R. Cech, *Annu. Rev. Biochem.* **59**, 543 (1990).
10. D. L. Robertson and G. F. Joyce, *Nature* **344**, 467 (1990).
11. D. Herschlag and T. R. Cech, *ibid.*, p. 405.
12. J. A. Piccirilli *et al.*, *Science* **256**, 1420 (1992).
13. F. Michel and E. Westhof, *J. Mol. Biol.* **216**, 585 (1990).
14. F. Michel *et al.*, *Genes Dev.* **6**, 1373 (1992).
15. J. F. Wang and T. R. Cech, *Science* **256**, 526 (1992).
16. A. M. Pyle, F. L. Murphy, T. R. Cech, *Nature* **358**, 123 (1992).
17. J. A. Latham and T. R. Cech, *Science* **245**, 276 (1989).
18. W. D. Downs and T. R. Cech, *Biochemistry* **29**, 5605 (1990).
19. J. F. Wang and T. R. Cech, unpublished data.
20. Guanosine 5′-phosphorothioate (GMPS) was synthesized by reaction of guanosine (Sigma) with thiophosphoryl chloride (Aldrich) in triethyl phosphate (Aldrich) [A. W. Murray and M. R. Atkinson, *Biochemistry* **7**, 4023 (1968)] (*21*). After purification by high-performance liquid chromatography (HPLC), the GMPS was used as the initiating nucleotide for transcription in vitro of L-21 Sca I RNA by bacteriophage T7 RNA polymerase as described (*8*), except that 4 mM GMPS and 0.25 mM GTP were used. Most studies were performed with [^{32}P]RNA, synthesized by inclusion of [α-^{32}P]ATP in the transcription reaction. RNA was purified by electrophoresis on a 6 percent polyacrylamide–7 M urea gel, visualized by autoradiography, eluted from the gel, precipitated with ethanol, and resuspended in 40 mM sodium bicarbonate (pH 8.5). A small volume of methanol saturated with azidophenacyl bromide was then added so that the final concentration of azidophenacyl bromide was 5 to 50 mM. After 1 hour at room temperature, excess azidophenacyl bromide was removed by extraction with two volumes of phenol and the 5′-azido L-21 Sca I RNA was recovered by ethanol precipitation.
21. A. B. Burgin and N. R. Pace, *EMBO J.* **9**, 4111 (1990).
22. G. B. Schuster, *NATO ASI SER., Ser. C* **272**, 31 (1989).
23. Because the efficiency of crosslinking could depend on distance from nitrene to crosslinking site, relative orientation and local motion of both groups, and the quantum yield, which could depend on the functional group being attacked by the nitrene, the yield of a crosslinked product may not accurately reflect the occupancy of a particular conformational state. However, the major crosslinks described in this article were produced with high efficiency for azido photo-crosslinks, providing some assurance that they represent the major conformers of the molecule.
24. B. Ruskin, A. R. Krainer, T. Maniatis, M. R. Green, *Cell* **38**, 317 (1984); P. J. Grabowski, R. A. Padgett, P. A. Sharp, *ibid.* **37**, 415 (1984).
25. C. A. Grosshans and T. R. Cech, *Biochemistry* **28**, 6888 (1989); D. W. Celander and T. R. Cech, *Science* **251**, 401 (1991).
26. $(k_{cat}/K_m)^S$ is the second-order rate constant for the reaction between the ribozyme-guanosine complex and the oligonucleotide substrate; for the uncrosslinked ribozyme, this rate constant is limited by k_{on}^S, the rate constant for the binding of the RNA substrate (*27*).
27. D. Herschlag and T. R. Cech, *Biochemistry* **29**, 10159 (1990).
28. Reverse transcriptase terminates DNA synthesis at the nucleotide immediately preceding a crosslink in the RNA template [O. Hagenbuchle, M. Santer, J. A. Steitz, R. J. Mans, *Cell* **13**, 551 (1978); R. Denman, J. Colgan, K. Nurse, J. Ofengand, *Nucleic Acids Res.* **16**, 165 (1988); (*18*)]. Hence the crosslink site is assigned as one nucleotide 5′ of the stop site of chain elongation. These stop points were not observed when primer extension was performed with the RNA that had been irradiated but had not become crosslinked (Fig. 3). The **2a** crosslink obtained with the DNA 5′ exon analogue bound to the ribozyme was mapped to the same location as that obtained with free ribozyme.
29. A. M. Pyle and T. R. Cech, *Nature* **350**, 628 (1991); P. C. Bevilacqua and D. H. Turner, *Biochemistry* **30**, 10632 (1991); D. Herschlag, F. Eckstein, T. R. Cech, in preparation.
30. A. M. Pyle, J. A. McSwiggen, T. R. Cech, *Proc. Natl. Acad. Sci. U.S.A.* **87**, 8187 (1990).
31. S. Couture *et al.*, *J. Mol. Biol.* **215**, 345 (1990); K. Williams, D. Fujimoto, T. Inoue, *Proc. Natl. Acad. Sci. U.S.A.* **89**, 10400 (1992).
32. K. Williams, D. Fujimoto, T. Inoue, personal communication.
33. D. Herschlag, *Biochemistry* **31**, 1386 (1992).
34. P. C. Bevilacqua, R. Kierzek, K. A. Johnson, D. H. Turner, *Science* **258**, 1355 (1992).
35. D. E. Koshland, Jr., *Proc. Natl. Acad. Sci. U.S.A.* **44**, 98 (1958); F. A. Quiocho and W. N. Lipscomb, *Adv. Protein Chem.* **25**, 1 (1971).
36. This conclusion could also be inferred in that all of the bound RNA oligonucleotide has the very slow dissociation rate characteristic of binding by both tertiary interactions and base pairing (*27*).
37. D. Herschlag, personal communication. The observations concern d(GGCCCUCUAAAAA). The open complex also being preferred with d(GGCCCUCU) bound is inferred from the similar K_d's of the complexes formed with these two deoxyoligonucleotides [see also (*33*)].
38. T. H. Kao and D. M. Crothers, *Proc. Natl. Acad. Sci. U.S.A.* **77**, 3360 (1980). K. A. LeCuyer and D. M. Crothers, *Biochemistry*, in press.
39. C. W. Pikielny, B. C. Rymond, M. Rosbash, *Nature* **324**, 341 (1986); S. C. Cheng and J. Abelson, *Genes Dev.* **1**, 1014 (1987); A. I. Lamond, M. M. Konarska, P. J. Grabowski, P. A. Sharp, *Proc. Natl. Acad. Sci. U.S.A.* **85**, 411 (1988); D. A. Wassarman and J. A. Steitz, *Science* **257**, 1918 (1992).

40. We thank A. Gooding for synthesis of oligonucleotides; J. Piccirilli, B. Hicke, and D. Herschlag for discussions; E. Christian, J. Doudna, and A. M. Pyle for comments on the manuscript. Supported by the Howard Hughes Medical Institute (J.-F.W. and T.R.C.) and the National Institutes of Health (W.D.D.). The W. M. Keck Foundation has provided generous support of RNA science on the Boulder campus.

5 January 1993; accepted 20 March 1993